Structural phase transition and T_c distribution in Hf-doped $LaMnO_3$ investigated using perturbed-angular-correlation spectroscopy

Gary L. Catchen
Department of Nuclear Engineering and Electronic Materials and Processing Research Laboratory, The Pennsylvania State University, University Park, Pennsylvania 16802

William E. Evenson and David Allred
Department of Physics, Brigham Young University, Provo, Utah 84602
(Received 28 March 1996)

Using perturbed-angular-correlation (PAC) spectroscopy, via the $^{181}Hf \rightarrow ^{181}Ta$ probe, we have measured Mn-site electric-field gradients (EFG's) at Ta nuclei in ceramic samples of $LaMnO_3$. Two crystallographic phases coexist over a temperature interval of ≈ 16 K near the orthorhombic-to-rhombohedral transition at ≈ 724 K, which shows a thermal hysteresis of $\approx 1.7 \pm 0.2$ K. Concurrently, in the two phases, we determined the temperature dependence of the EFG parameters, V_{zz}, η, and δ, and the ratio of the probe concentrations A_1/A_2. To explain the apparent coexistence of two phases in this weakly first-order transition, we present a model that assumes a spatial distribution of T_c values. This distribution could arise from a spatially nonuniform distribution of Mn^{4+} ions. We show the PAC technique to be a uniquely powerful probe of local symmetries that reflect the effects of a local distribution of valences, which drive the phase transition. [S0163-1829(96)52230-7]

During the past several decades, scientists have investigated phase transitions in many technologically important perovskites, and they primarily have used macroscopic properties such as heat capacities, susceptibilities, and diffraction-derived parameters to quantitatively characterize these transitions. By their very nature, these quantities represent gross averages over the atomic-scale properties of crystals. New detailed atomic-scale information may lead to a better understanding of phase transitions. For this purpose, we use the perturbed-angular-correlation (PAC) technique to sample local environments on the scale of a few atomic lengths, so that we can observe small regions of different phases and thereby infer local variations in transition temperature.

PAC spectroscopy provides this type of detailed information via measurements of magnetic hyperfine fields and electric-field gradients (EFG's) at a specific site in the crystal. For this purpose, a relatively small amount of a radioactive PAC probe ion, $^{181}Hf \rightarrow ^{181}Ta$, is substituted into a site in the crystal. The hyperfine interaction of the probe's nuclear electric-quadrupole moment (for the case reported here) and the extranuclear EFG perturbs the spatial and temporal correlations of the γ rays emitted by ^{181}Ta excited nuclei after the radioactive decay of ^{181}Hf. A recent review provides more information about PAC spectroscopy.[1]

The approach, therefore, is to measure the parameters that describe the hyperfine interaction, while a crystal undergoes a phase transition. However, generally, these hyperfine parameters need not be connected *a priori* in a direct way to macroscopic thermodynamic quantities. The connection between spectroscopic and thermodynamic quantities must be made by creating a consistent picture using all available evidence, which includes both macroscopic measurements and hyperfine parameters. To demonstrate this approach, we have measured the Mn-site EFG in Hf-doped $LaMnO_3$ during an elevated-temperature structural phase transition, and we have observed the coexistence of two phases over a range of temperatures, which we interpret using a model that includes a spatial distribution of critical temperature T_c values. This distribution implies that this perovskite material has a Mn valence that varies on a nanometer scale.

The compound $LaMnO_3$ crystallizes in a perovskite structure.[2–5] We use the symbol ''$LaMnO_3$'' as shorthand for the formula $(LaMn^{3+}_{1-x}Mn^{4+}_x)O_3$, which indicates that the actual composition depends strongly on the Mn oxidation state. Depending on the processing conditions, several percent to several tens of percent of the manganese ions can have a 4+ oxidation state, and the formation of cation La^{3+} and Mn^{3+} vacancies is expected to compensate for the increased charge of the Mn^{4+} ions as well as the much-smaller concentration of Hf^{4+} probe ions.[5,6] Most reports indicate that, when $LaMnO_3$ ceramics are sintered under reducing conditions at high temperatures, the laboratory-temperature crystal has orthorhombic symmetry $Pbnm(D^{16}_{2h})$ and the composition is nearly stoichiometric.[4]

An early investigation[2] indicates that the crystal undergoes a transition to a rhombohedral structure at ≈ 870 K when the Mn^{4+}-ion concentration is near zero. As the Mn^{4+}-ion concentration increases, the transition temperature decreases. The Mn^{4+} ionic radius (0.68 Å)[7] is smaller than the Mn^{3+} ionic radius (0.785 Å),[7] and the rhombohedral structure has a smaller unit-cell volume than the orthorhombic structure has. So the smaller ion introduces lattice strains that favor the rhombohedral structure. The Hf^{4+} probe ion, which substitutes into the Mn site, has an ionic radius of 0.85 Å .[7] Although trace amounts of Hf^{4+} PAC probes may introduce some lattice strains, the symmetry of the EFG at any probe site will be determined by the larger local environment. The concentration of Hf probes is so small that the probes will negligibly affect the observed transition temperature in this experiment.

Ceramic samples of $LaMnO_3$ were prepared using a resin-intermediate method, which involved the metal precursors, $La(OH)_3$ and $Mn(CH_3COO)_3$, and the Hf concentration was ≈ 0.07 at. % of the Mn concentration. The resulting powder of mixed oxides was pressed into small pellets and sintered at ≈ 1770 K under flowing Ar gas for 15–30 min. Subsequently, the samples were crushed and sealed into small fused-silica tubes; one sample was sealed under air and another was sealed under Ar gas. X-ray powder diffraction patterns were measured on small amounts of the radioactive powder and the samples were found to be phase pure to within several percent.

The experimental time distributions were measured using a four-BaF_2-detector PAC spectrometer, which has a time resolution of ≈ 800 psec full width at half maximum. A specially-designed furnace and temperature control system was used to maintain the samples at constant temperature, ± 0.03 K, during the measurement periods of 0.5–1 day. Also the controller was adjusted to avoid significant overshoots and undershoots when the sample temperature was either increased or decreased. The measured perturbation functions $A_{22}G_{22}(t)$ were analyzed using a two-site model for static nuclear-electric-quadrupole interactions:

$$-A_{22}G_{22}(t) = \sum_{j=1}^{2} A_j \left[S_0 + \sum_{k=1}^{3} S_k \exp(-\delta_j \omega_{jk} t) \cos(\omega_{jk} t) \right] + A_3 . \quad (1)$$

Here A_1 and A_2 are the normalization factors, δ_1 and δ_2 are the Lorentzian line-shape parameters that correspond to static linebroadening, and A_3 takes into account both the effects of γ rays that are absorbed by the sample en route to the detectors and the fraction of probe atoms that are not in a well-defined chemical environment. (For most of the measurements reported here $A_3 \approx 0$, because the samples were relatively small.) The site-occupancy fractions are represented by $f_i = A_i/(A_1+A_2+A_3)$, $i=1$, 2. The nonvanishing EFG components V_{ii} in the principal-axis system where the probe nucleus is at the origin are related to the quadrupole frequency and asymmetry parameter by $\omega_Q = eQV_{zz}/4I(2I-1)\hbar$ and $\eta = (V_{xx}-V_{yy})/V_{zz}$ in which Q represents the nuclear electric-quadrupole moment (2.51 b) for the ^{181}Ta spin $I=5/2$ intermediate level.

Figure 1 presents several representative perturbation functions out of those that were measured at temperatures near T_c. The 733.7-K perturbation function represents an interaction that occurred at a single site in the higher-temperature phase, and the 716.2-K perturbation function represents an interaction that occurred at a single site in the lower-temperature phase. At in-between temperatures, the perturbation functions represent two interactions that correspond to the probe sites in the two phases.

In addition, Fig. 1 presents two perturbation functions measured at laboratory temperature; the first was measured initially and the second was measured after the long series of measurements at temperatures near T_c was completed. The EFG parameters that were obtained from the fits of these two laboratory-temperature perturbation functions agree well and indicate that primarily one interaction took place at a single site. The average parameter values are $\omega_Q = 158.5 \pm 0.5$ Mrad sec^{-1}, $\eta = 0.83 \pm 0.01$, and $\delta = 0.027 \pm 0.002$. In $LaMnO_3$ interstitial O^{2-} ions and cation vacancies are the dominant types of point defects.[5] If either defect type were to reside near some of the probe ions, either multiple interactions, or linebroadening, or both could occur. These effects are not strongly evident in our PAC measurements for samples that were initially sintered under Ar gas and not subsequently annealed in air at temperatures above ≈ 800 K. These defect effects are evident; however, in the measurements that were performed either while or after the samples were annealed at higher temperatures in air. These observa-

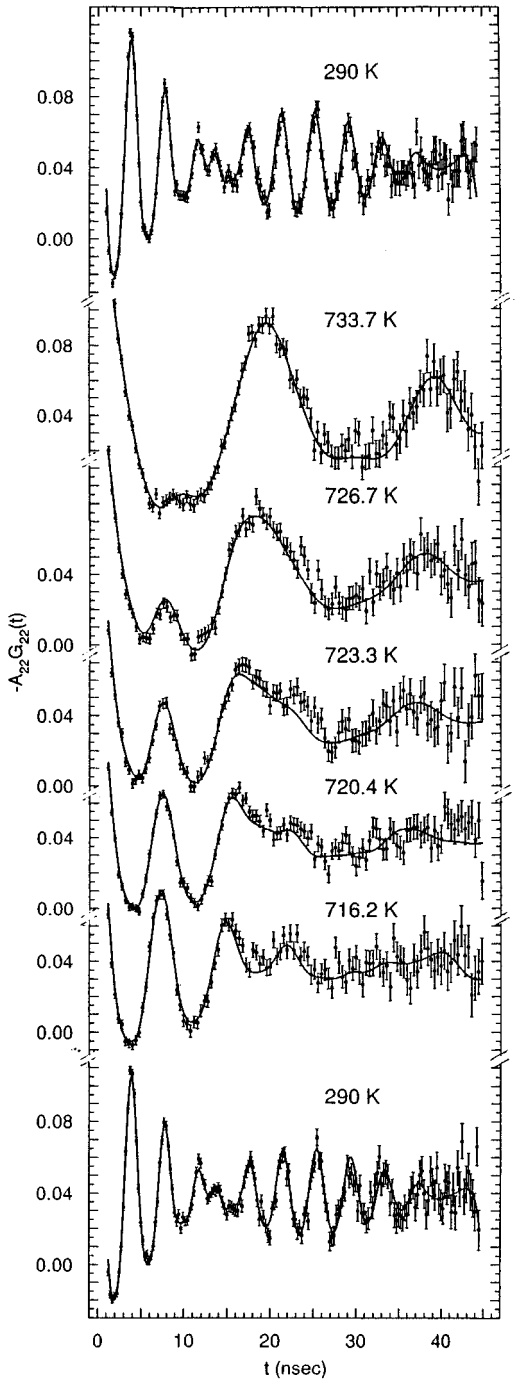

FIG. 1. Several representative perturbation functions that were measured on a ceramic sample of $LaMnO_3$ at the indicated temperatures. The solid lines represent fits of Eq. (1) to the data points.

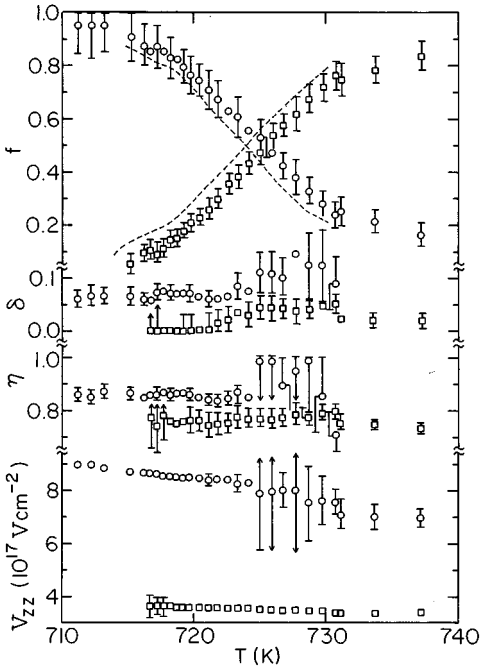

FIG. 2. Summary of parameters derived from fits of Eq. (1) to the experimental data points. The circles correspond to the interactions measured in the low-temperature phase, and the squares correspond to the interactions measured in the high-temperature phase. The measurements that these parameters correspond to were performed at *successively increasing* temperatures. The dashed line shown in the site-occupancy fraction temperature dependence represents the f values measured at *successively decreasing* temperatures. The displacement of this dashed line to lower temperatures indicates that thermal hysteresis $\Delta T = 1.7$ K characterizes the transition.

tions indicate that the very high-temperature sintering of $LaMnO_3$ under Ar gas therefore produces samples that have close to stoichiometric oxygen content, i.e., $x \approx 0$. However, the small-but-nonvanishing laboratory-temperature δ values suggest that the crystals contain some defects as a result of the presence of small Mn^{4+}-ion concentrations.

To assign the site substitution of the $^{181}Hf \rightarrow {}^{181}Ta$ probe, we used the initial results of PAC measurements performed at cryogenic temperatures (≈ 140 K), where $LaMnO_3$ orders magnetically.[8] In structurally-related magnetic ABO_3 perovskites such as $LaFeO_3$, a very large supertransferred magnetic hyperfine field can occur at the B site.[9] At the corresponding A site, these supertransferred fields tend to be minuscule.[9] The cryogenic-temperature PAC measurements indicate the presence of relatively large magnetic hyperfine fields at the $^{181}Hf \rightarrow {}^{181}Ta$ probe site.[8] At $T \ll T_c$, the large observed Larmor frequency ω_L (Ref. 8) indicates that the ^{181}Hf probe substitutes for Mn in $LaMnO_3$.

Figure 2 summarizes the parameters derived from a series of measurements performed at temperatures near T_c. In this series, the temperature was increased before each successive measurement. The V_{zz} values are much lower and the η values are somewhat lower for the higher-temperature phase than those for the lower-temperature phase. This trend is consistent with the qualitative expectation that, at higher temperatures, the stable phases tend to be more symmetrical and, as such, they should be characterized by lower V_{zz} and η values. We expect the η values for the rhombohedral phase to be close to zero, because the structure has a threefold rotational axis at the Mn site. Instead, however, the higher-temperature phase shows η values that range from 0.7 to 0.8. One possible explanation for this discrepancy is that the higher-temperature phase was incorrectly identified as having rhombohedral symmetry. Another possibility is that the Hf^{4+}-probe ion traps a defect because it differs in charge and size from the indigenous Mn^{3+} ions. To test the latter hypothesis, PAC measurements should be performed in which the O_2 partial pressure is varied at several specific elevated temperatures, >800 K. In the absence of this information, we cannot say more about this interesting phenomenon.

The site-occupancy fractions f_1 and f_2 show smooth monatonic changes as the temperature increases. A similar series of measurements was performed on the same sample, as it was cooled through the transition. The f_1 and f_2 values show very similar patterns, except that the data points are shifted about 1–2 K to lower temperatures. This result indicates that thermal hysteresis is operative during this transition. When $f_1 = f_2 = 0.5$, the curves are separated by $\Delta T = 1.7 \pm 0.2$ K, which represents the thermal hysteresis for this experiment. This 1.7 K of hysteresis was determined by moving through the 16 K temperature interval in steps of typically 0.5 K and collecting data for 8–14 h at each step before changing the temperature by another 0.5 K.

For metal-oxide crystals, structural phase transitions can be categorized as being either first-order or continuous.[10] A first-order transition is characterized by a discontinuity at the transition temperature T_c in one of the first derivatives of the Gibbs free energy, such as in either the volume or the entropy. The order parameter for a continuous transition decreases continuously and reaches zero as the temperature approaches T_c from below, and the derivative(s) of the order parameter may become discontinuous at T_c. Often in continuous transitions, the crystal symmetries below and above T_c are similar; neither thermal hysteresis nor a latent heat are observed; and the transition occurs between contiguous states in the thermodynamic configuration space. Thus, first-order and continuous transitions have distinctly different features. However, when the crystal symmetries and the latent-heat and thermal-hysteresis magnitudes differ very little, the experimental distinction between these two types of transitions may be difficult to discern.

The observed transition in $LaMnO_3$ shows the characteristics of a weakly first-order transition; namely, two distinctly different sets of EFG parameters characterize the two phases and a small amount of thermal hysteresis accompanies the transition. However, both phases appear to coexist over a temperature range of approximately 16 K. This range of coexistence is too large to be explained by temperature drifting in the sample during measurement. Furthermore, first-order transitions occur at a definite temperature, with hysteresis coming only from nucleation and growth energies, superheating and supercooling, etc. Therefore, we suggest that a distribution of T_c values characterizes the sample. To evaluate this possibility, we first further analyze the site-occupancy information. We define the ratio $[f/(1-f)] = (A_1/A_2)$, which represents the ratio of the

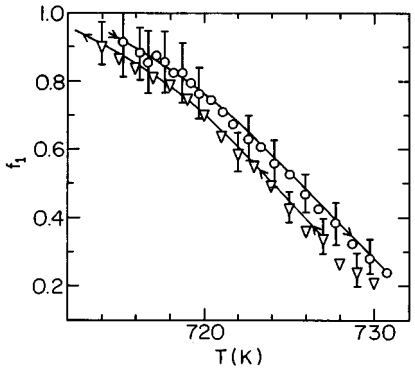

FIG. 3. Site occupancy fractions for the orthorhombic phase. The circles represent the PAC data for successively increasing temperatures, and the triangles represent the data for successively decreasing temperatures. The lines represent fits of Eq. (2) to the data.

probe concentration in the lower-temperature phase to the probe concentration in the higher-temperature phase.

If the transition temperature varies within the sample because a nonuniform spatial distribution of Mn^{4+} ions is present, then different Hf probe nuclei will experience the symmetry change associated with the transition at different sample temperatures. As a simple model of this phenomenon, we assume that the distribution of transition temperatures experienced by the various PAC probe nuclei is Gaussian, characterized by mean transition temperature T_c and standard deviation σ. Using this model, the fraction of probes whose immediate neighborhood is in the high-temperature phase, i.e., $(1-f)$, at temperature T is given by the probability that the transition temperature for the local neighborhood is $\leqslant T$. Using the Gaussian distribution of local transition temperatures, this probability is just the cumulative distribution function:

$$1-f=\int_{-\infty}^{T} P(\tau)\,d\tau=\frac{1}{2}\{1+\mathrm{erf}[(T-T_c)/(\sqrt{2}\sigma)]\}. \quad (2)$$

For the temperature-increasing set of measurements, the fits give $T_c=723.8\pm0.1$ K and $\sigma=7.4\pm0.1$ K. For the temperature-decreasing set, the fits give $T_c=725.5\pm0.2$ K and $\sigma=7.3\pm0.3$ K. Figure 3 shows fits of Eq. (2) to the site-occupancy fractions for the lower-temperature phase for both temperature-increasing and temperature-decreasing sets of measurements. The values for the higher-temperature phase show corresponding behavior.

The more important question is what causes the variation in local T_c values. We have suggested that this variation is caused by a nonuniform spatial distribution of Mn^{4+} ions. There will be some number of Mn^{4+} ions in the material to compensate cation vacancies or oxygen interstitials introduced during processing. The presence of an Mn^{4+} ion may introduce local strains in the neighborhood of that ion because it has a smaller size compared to the Mn^{3+} ions. In the region over which these strains extend, i.e., a few atomic distances from the Mn^{4+} ion, the strain energy favors the rhombohedral structure and allows the phase transition to proceed in that local region at a temperature slightly lower than the mean transition temperature for the entire sample. If the Mn^{4+} ions were distributed uniformly through the sample, in sufficient density that the strain fields overlapped throughout, then we would expect to observe no variation in the transition temperature from place to place within the sample. However, the Mn^{4+} ions are only present in very low concentrations, so we observe statistical variations in their local concentration. Because the concentrations are small and the variation in transition temperature is small, we should be able to make a linear approximation for the relationship between transition temperature and Mn^{4+} concentration. Hence, random variations in Mn^{4+} concentration in the neighborhood of different PAC probe nuclei should translate well to a Gaussian distribution for the local phase transition temperature. This distribution of local transition temperatures then gives rise to the coexistence of two phases that we observe.

In conclusion, we have measured the temperature dependence of the probe site-occupation fractions at temperatures near T_c that characterize the $LaMnO_3$ rhombohedral-to-orthorhombic transition. A model that describes the transition using a Gaussian distribution of T_c values provides a good representation of the site-occupancy temperature dependence. This result implies that spatial fluctuations in the local environment are responsible for the coexistence of two phases during this first-order transition. This result demonstrates that PAC measurements can be used to obtain new, important information about phase transitions in complex metal oxides.

We thank Professor Darrell G. Schlom of the Department of Materials Science and Engineering of Pennsylvania State University, who contributed much knowledge and expertise about materials properties. We thank Todd M. Rearrick, who designed and built the furnace and temperature-control system. We thank the Office of Naval Research for partial support via Grant No. N0014-90-J-4112.

[1] G. L. Catchen, MRS Bull. **20**, 37 (1995).

[2] A. Wold and R. J. Arnott, J. Phys. Chem. Solids **9**, 176 (1959).

[3] G. Matsumoto, J. Phys. Soc. Jpn. **29**, 606 (1970).

[4] J. B. A. Elemans, B. Van Laar, K. R. Van der Veen, and B. O. Loopstra, J. Solid State Chem. **3**, 238 (1971); W. C. Koehler and E. O. Wollan, J. Phys. Chem. Solids **2**, 100 (1957).

[5] B. C. Tolfield and W. R. Scott, J. Solid State Chem. **10**, 183 (1974).

[6] G. J. McCarthy, P. Y. Gallagher, and C. Sipe, Mater. Res. Bull. **8**, 1277 (1993).

[7] R. O. Shannon and C. T. Prewitt, Acta Crystallogr. Sect. B **26**, 1046 (1970).

[8] R. L. Rasera, G. L. Catchen, and T. M. Rearick, *Proceedings of the 10th International Conference on Hyperfine Interactions*, Leuven, Belgium, 1995, edited by M. Rots, A. Vantomme, J. Dekoster, R. Coussement, and G. Langouche (J. C. Baltzer AG, Science Publishers, Basel, Switzerland, 1995), pp. 127–130.

[9] T. M. Rearick, G. L. Catchen, and J. M. Adams, Phys. Rev. B **48**, 224 (1993)

[10] H. B. Callen, *Thermodynamics and an Introduction to Thermostatistics*, 2nd ed. (Wiley, New York, 1985), pp. 215–276.